Hole distribution in $(Tl_{0.5}Pb_{0.5})Sr_2(Ca_{1-x}Y_x)Cu_2O_7$ studied by x-ray absorption spectroscopy

J. M. Chen
Synchrotron Radiation Research Center (SRRC), Hsinchu, Taiwan, Republic of China

R. S. Liu
Department of Chemistry, National Taiwan University, Taipei, Taiwan, Republic of China

W. Y. Liang
Interdisciplinary Research Center in Superconductivity, University of Cambridge, Cambridge, United Kingdom
(Received 12 April 1996; revised manuscript received 10 June 1996)

High-resolution O K-edge and Cu L_{23}-edge x-ray-absorption near-edge-structure spectra for the series of $(Tl_{0.5}Pb_{0.5})Sr_2(Ca_{1-x}Y_x)Cu_2O_7$ compounds ($x=0$–0.9) were measured using a bulk-sensitive total-fluorescence-yield technique. Near the O $1s$ edge, a well-pronounced pre-edge peak with maxima at ~528.3 eV is observed, which is ascribed to the excitations of O $1s$ electrons to O $2p$ holes located in the CuO_2 planes. The intensity of this pre-edge peak increases linearly with the Ca doping for $0 \leqslant x \leqslant 0.5$. This indicates that the effect of chemical substitution of Ca^{2+} for Y^{3+} is to induce hole states in the CuO_2 planes near the Fermi level, which are important to control the T_c for the series of $(Tl_{0.5}Pb_{0.5})Sr_2(Ca_{1-x}Y_x)Cu_2O_7$ compounds. Moreover, the generation of holes in the O $2p$ orbitals within the CuO_2 planes is probably responsible for inducing a transition from a semiconductor to a superconductor. In the Cu L-edge absorption spectra, high-energy shoulders at 933.1 and 952.9 eV are assigned to the transitions from the $Cu(2p_{3/2,1/2})3d^9L$ ground state to the $Cu(2p_{3/2,1/2})^{-1}3d^{10}L$ excited state, where L denotes the O $2p$ ligand hole. The normalized intensity of these defect states shows a linear increase with increasing the chemical concentration of Ca in the Y sites. [S0163-1829(96)05341-6]

I. INTRODUCTION

Following the discovery of the new high-temperature superconductors, there has been a massive research effort to understand the mechanism of superconductivity. It has been experimentally demonstrated that holes are responsible for superconductivity from the correlation between the superconducting transition temperature (T_c) and the hole concentration.[1] A precise knowledge of the unoccupied electronic structure near the Fermi level of these compounds is therefore an important first step toward comprehensive understanding the electronic states of holes and the mechanism of superconductivity. For this reason, direct experimental information on the electronic structures of these compounds is of particular importance. For years, absorption spectroscopy techniques, such as high-energy electron-energy-loss spectroscopy (EELS) and x-ray-absorption spectroscopy, have been widely applied to probe the unoccupied density of states near the Fermi level in the high-T_c superconductors.[2–4] X-ray-absorption near-edge structure (XANES) is a modern tool for the investigation of the electronic states at a selected site in complex materials. The availability of dedicated third-generation synchrotron radiation x-ray sources make it feasible to measure high-signal-to-noise-ratio and high-resolution absorption spectra.

The occurrence of superconductivity adjacent to a metal-insulator boundary is a characteristic feature of many high-T_c superconducting cuprate systems, e.g., $La_{2-x}Sr_xCuO_4$, $YBa_2Cu_3O_{1-\delta}$, and $Bi_2Sr_2Ca_{1-x}Y_xCu_2O_8$.[5–7] As yet, the precise mechanism of high-temperature superconductivity has not been delineated. However, a system exhibiting a composition-induced metal-superconductor-insulator transition offers a great potential for investigating the important structural and electronic characteristic which can lead to superconductivity at such extraordinary high temperature. One of such systems is the so-called Tl-based septenary cuprate $(Tl_{1-y}Pb_y)Sr_2(Ca_{1-x}Y_x)Cu_2O_7$, hereafter referred to as Tl-1212, where both x and y can be varied. The structure of the Tl-1212 phase $(Tl_{0.5}Pb_{0.5})Sr_2(Ca_{1-x}Y_x)Cu_2O_7$ can be described in terms of an intergrowth of double rocksalt-type layers [({Tl/Pb}O)(SrO)] with double $[Sr(Ca,Y)Cu_2O_5]$ oxygen-deficient perovskite layers,[8] formed by sheets of corner-sharing CuO_5 pyramids interleaved with calcium and/or yttrium ions as illuminated in Fig. 1.

This septenary system has the highest T_c among the thallium cuprate systems with the so-called 1212 structure. Typically, this structure sustains $T_c \sim 80$ K in the phases $(Tl_{0.5}Pb_{0.5})Sr_2CaCu_2O_7$ and $TlSr_2(Ca,Y)Cu_2,O_7$. However, the parent compound $TlSr_2CaCu_2O_7$ is itself a metal, but exhibits no superconductivity at temperatures down to 4 K. Such a conduction can be efficiently modified chemically by the stepwise substitution of Tl^{3+} by Pb^{4+}, by the substitutions of Ca^{2+} by Y^{3+}, or, indeed, by the dual substitutions Tl^{3+}/Pb^{4+}, Ca^{2+}/Y^{3+}. In Fig. 2 we show the T_c as a function of the compositional parameter x in $(Tl_{0.5}Pb_{0.5})Sr_2(Ca_{1-x}Y_x)Cu_2O_7$ compounds.[9] This system exhibits superconductivity over the homogeneity range $x=0$–0.5, with the superconducting transition temperature showing a maximum of 108 K at $x=0.2$. However, towards the high end of the Ca doping, the T_c of these compounds decreases which leads to a dome-shaped curve as shown in Fig. 2.

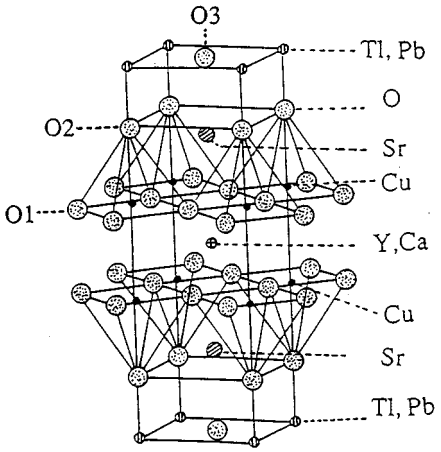

FIG. 1. A schematic representation of the crystal structure of $(Tl_{0.5}Pb_{0.5})Sr_2(Ca_{1-x}Y_x)Cu_2O_7$. Oxygen in the CuO_2 planes, apical sites, and (Tl,Pb)-O planes are denoted by O1, O2, and O3, respectively.

Across the homogeneity range $x=0.6$–1.0, the material also undergoes a metal-insulator transition at temperature above T_c. The great attraction of such materials is able to control the hole concentration in the CuO_2 sheets with a simple chemical substitution involving other layers in the unit cell. Based on our neutron-diffraction measurements, the oxygen stoichiometry across the series of $(Tl_{0.5}Pb_{0.5})Sr_2(Ca_{1-x}Y_x)Cu_2O_7$ remains unchanged.[10] This had an advantage over some measurements which the oxygen content is varied, because the disorder at oxygen sites makes it difficult to distinguish changes in the electronic structure.

In this paper we report soft-x-ray-absorption measurements at the O K edge and Cu L edge in the series of $(Tl_{0.5}Pb_{0.5})Sr_2(Ca_{1-x}Y_x)Cu_2O_7$ samples with x between 0 and 0.9 using a bulk-sensitive fluorescence-yield-detection method. Although the electronic structures of these materials have been measured by the EELS technique, the energy resolution in those studies is only about 1 eV.[11] Therefore, the detailed electronic structure near the Fermi level may have been lost. Our aim in this paper is to understand the variation of electronic structure of composition-induced insulator-superconductor-metal transition. The results reported here may be able to stimulate further experiments and theories, since this system offers a remarkable opportunity of testing and evaluating a theory of high-temperature superconductivity.

II. EXPERIMENTS

Samples with nominal compositions of $(Tl_{0.5}Pb_{0.5})Sr_2(Ca_{1-x}Y_x)Cu_2O_7$ ($x=0$–1) were prepared by the solid-state reaction method which has been reported in detail elsewhere, and so only pertinent details will be given here.[9] Samples in the whole composition range were prepared by mixing and grinding high-purity powders of $CaCO_3$, Y_2O_3, $SrCO_3$, and CuO in the appropriate stoichiometric proportions. The mixtures were calcined at 970 °C for 12 h in air to form a precursor. The precursor was mixed stoichiometric proportions Tl_2O_3 and PbO, and then ground

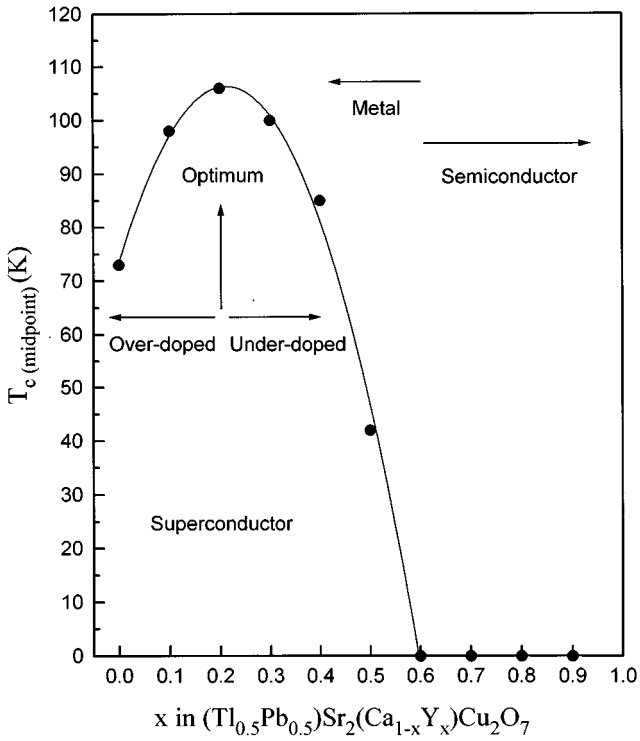

FIG. 2. Dependence of the superconducting transition temperature T_c as a function of compositional parameter x in $(Tl_{0.5}Pb_{0.5})Sr_2(Ca_{1-x}Y_x)Cu_2O_7$.

and pressed into a cylindrical pellet. The pellets were then wrapped in gold foil to prevent loss of thallium and lead during heating process. Subsequently, the samples were sintered at 950 °C for 3 h in flowing oxygen, followed by cooling to room temperature at a rate of 2–5 °C/min. The series of materials are single phase as checked by x-ray diffraction (XRD), neutron-diffraction, and energy-dispersive x-ray (EDX) spectroscopies.

In the x-ray-absorption measurements, each sintered sample was crushed into powder form. The resulting powder was glued onto a carbon-based conducting tape. The XANES measurements were carried out on the 6-m high-energy spherical grating monochromator (HSGM) beam line of the Synchrotron Radiation Research Center (SRRC) in Taiwan. The x-ray-fluorescence yield spectra were obtained using a microchannel plate (MCP) detector.[12] This MCP detector consists of a dual set of MCP's (25-mm diameter) with an electrically isolated grid mounted in front of them. For x-ray-fluorescence detection, the grid was set to a voltage of 100 V, while the front of the MCP's was set to −2000 V and the rear to −200 V. The grid bias ensured that positive ions would not be detected while the MCP bias ensured that no electrons were detected. The collector was set at ground potential and its output was detected using analog mode or standard pulse-counting techniques. The MCP detector was located ~2 cm from the sample and oriented parallel to the sample surface. Photons were incident at an angle of 45° with respect to the sample normal. The reference beam intensity (I_0) was measured simultaneously by a Ni mesh with 80% transmission. All the measurements were normalized to I_0. The photon energies were calibrated within accuracy of

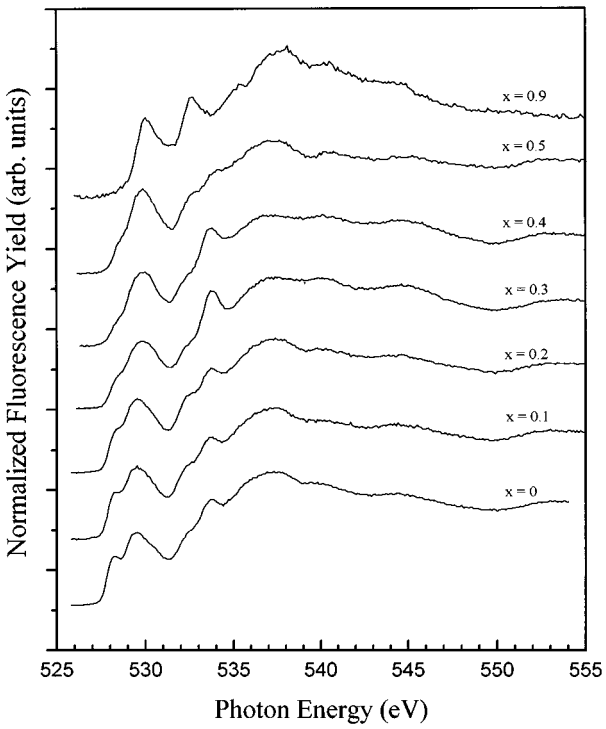

FIG. 3. O *K*-edge x-ray-absorption near-edge-structure spectra for the series of $(Tl_{0.5}Pb_{0.5})Sr_2(Ca_{1-x}Y_x)Cu_2O_7$ compounds with $x=0$, 0.1, 0.2, 0.3, 0.4, 0.5, and 0.9 by measuring the total-x-ray-fluorescence yield. These spectra have been normalized to have the same height at the main peak of 537 eV.

0.1 eV using the O *K*-edge absorption peak at 530.1 eV and Cu L_3 white line at 931.2 eV of CuO compound. To obtain the high-resolution spectra, the energy resolution of the monochromator was set to ~0.25 and ~0.5 eV at O 1*s* and Cu 2*p* absorption edges, respectively. All the measurements were done at room temperature.

III. RESULTS AND DISCUSSION

A. O *K*-edge XANES

In Fig. 3 high-resolution O *K*-edge x-ray-absorption near-edge structure (XANES) spectra for the series of $(Tl_{0.5}Pb_{0.5})Sr_2(Ca_{1-x}Y_x)Cu_2O_7$ samples ($x=0$–0.9) in the energy range of 526–555 eV are shown by measuring the total x-ray-fluorescence yield. It has been demonstrated that in the cuprate superconductors the discrete resonant absorption dominates the multiple-scattering modulation to the x-ray-absorption near-edge regime. In the first-order approximation, the multiple-scattering effect in the XANES spectrum can be neglected. The XANES can be regarded as a direct probe of the local density of unoccupied states close to the Fermi level at the excited atom. Dipole selection rules apply for small momentum transfer. Therefore, in the oxygen *K*-edge x-ray-absorption spectrum measurement, the unoccupied states with the mainly O 2*p* character are probed.

The O *K*-edge x-ray-absorption spectrum for the sample with $x=0.9$, as seen from Fig. 3, mainly consists of a peak at ~530 eV and a broad peak at ~537 eV. As determined by inverse photoemission experiments, the Sr empty *d* states as well as other empty *d* states of Ca and Y are all located at least about 5–10 eV above the Fermi level.[13] Therefore, the transitions from O 1*s* core level to these empty *d* states hybridized with O 2*p* states are more likely to be responsible for the main absorption peak at ~537 eV in Fig. 3. The XANES spectra for various compounds with different *x* values, as shown in Fig. 3, were normalized to have the same height at the main peak of 537 eV.

As the Ca doping increases, this gives rise to a new pre-edge feature at ~528.3 eV for $x\leqslant 0.5$. In addition, this pre-edge peak for $x=0$ in Fig. 3 shifts by 0.1–0.2 eV to higher energies as the increase of the Y content. This indicates that the effect of chemical substitution of Ca^{2+} for Y^{3+} is to induce hole states with the O 2*p* character near the Fermi level. In this respect, the compounds are typical of a *p*-type cuprate superconductor.[14,15] Liu and Edwards have measured the Hall number per Cu at room temperature for these compounds versus Ca concentration.[16] They observed a monotonic increase in the Hall number with a decrease in the compositional parameter *x*. This data gives an evidence in support of our observation.

Based on the recent studies of electronic structures in the $HgBa_2CuO_{4+\delta}$ (Hg-1201), $HgBa_2CaCu_2O_{6+\delta}$ (Hg-1212), and $HgBa_2Ca_2Cu_3O_{8+\delta}$ (Hg-1223) compounds by Pellegrin *et al.*,[17] they have assigned the low-energy excitation at about 528.2 eV to O 2*p* hole states in the O(1) and O(1′) sites within the CuO_2 planes. This assignment was supported by the polarization-dependent XANES measurements on single-crystalline $HgBa_2Ca_3Cu_4O_{10+\delta}$.[17] Furthermore, according to the x-ray photoelectron spectroscopy measurements on the O 1*s* core levels of epitaxial Hg-1212 films, the O 1*s* binding energy in the O(1) site is smaller than that in the O(2) sites.[18] In the crystal structure of $(Tl_{0.5}Pb_{0.5})Sr_2(Ca_{1-x}Y_x)Cu_2O_7$ (Tl-1212), it consists of three nonequivalent oxygen sites, O(1) in the CuO_2 layers, O(2) in the apical oxygen sites, and O(3) in the (Tl,Pb)-O planes, as illuminated in Fig. 1. Such a structure is similar to that of $Hb_2Ba_2CaCu_2O_{6+\delta}$ (Hg-1212) having a $P4/mm$ space group and lattice constants of $a\sim 3.8$ Å and $c\sim 12$ Å.[16] In analogy to results from other *p*-type cuprate superconductors,[4,7] the pre-edge peak at ~528.3 eV in Fig. 3 for the series of $(Tl_{0.5}Pb_{0.5})Sr_2(Ca_{1-x}Y_x)Cu_2O_7$ samples can be ascribed to the excitations of O 1*s* electrons to O 2*p* holes located in the CuO_2 planes. As seen from Fig. 3, the intensity of this pre-edge peak increases with increasing the Ca doping. A similar behavior in the oxygen 1*s* absorption spectra against the hole concentration was reported for the $La_{2-x}Sr_xCuO_4$, $YBa_2Cu_3O_{7-\delta}$, and $Bi_2Sr_2Ca_{1-x}Y_xCu_2O_8$ compounds.[7,19–22]

For most of cuprate superconductors, the lowest binding energies for the oxygen 1*s* states have been found to be between 528.5 and 529.0 eV.[23,24] It is reasonable to assume that the lowest binding energies for the O 1*s* state in the titled compounds are also in the same range. In addition, the core-hole effect in O 1*s* absorption spectrum can be neglected. This assumption is supported by the strong similarity of O 1*s* absorption spectra and resonant high-energy inverse photoemission spectra on $Bi_2Sr_2CaCu_2O_8$.[25] Therefore, the broad peak at ~530 eV in O *K*-edge absorption spectrum indicates that above the semiconducting gap, the conduction-band states must have considerable oxygen 2*p* character.

According to band-structure calculations, electron pockets at the *T* and *Z* points of the Brillouin zone are formed from

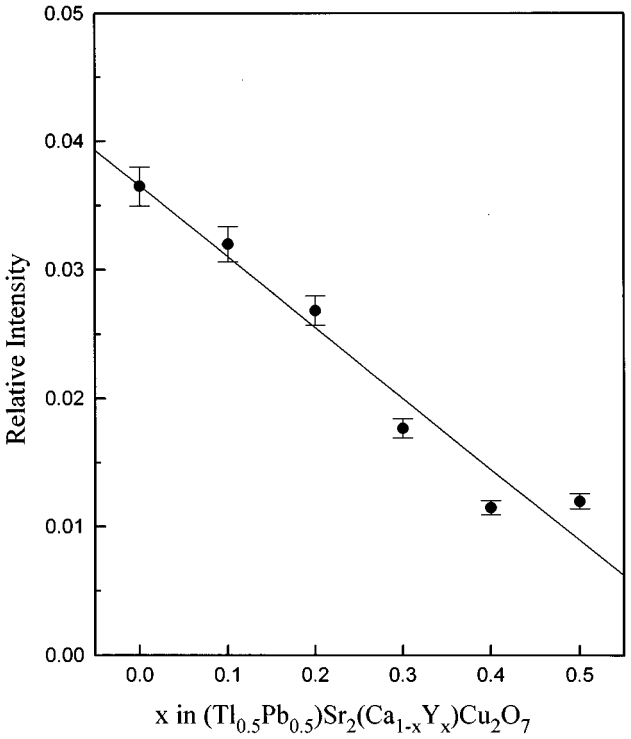

FIG. 4. Dependence on compositional parameter x in $(Tl_{0.5}Pb_{0.5})Sr_2(Ca_{1-x}Y_x)Cu_2O_7$ of relative intensity of the pre-edge peak at ~528.3 eV corresponding to the O $2p$ holes from the CuO_2 planes. The curves are drawn as a guide for the eyes.

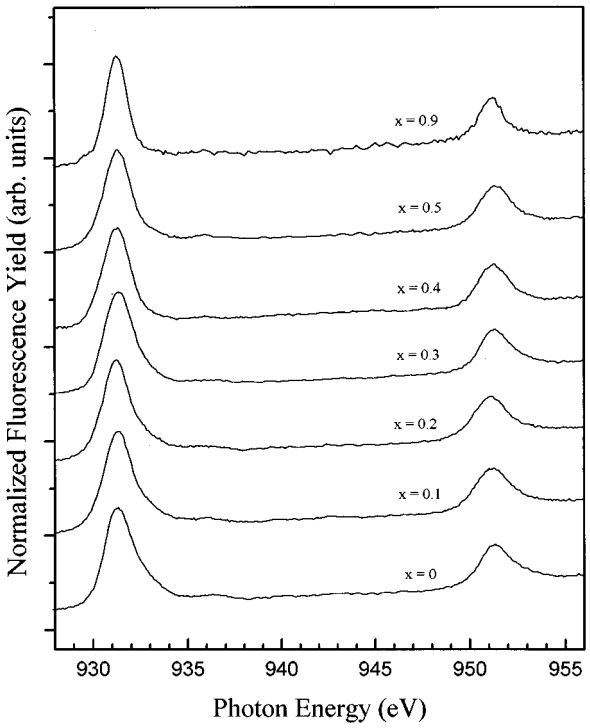

FIG. 5. Copper L_{23}-edge x-ray-absorption spectra for the series of $(Tl_{0.5}Pb_{0.5})Sr(Ca_{1-x}Y_x)Cu_2O_7$ compounds with $x=0$, 0.1, 0.2, 0.3, 0.4, 0.5, and 0.9.

an antibonding band composed of O(2) $2p$ (in the BaO planes) and O(3) $2p$ orbitals (in the TlO planes) hybridized with Tl $6s$ and Tl $5d_{3z^2r^2}$ orbitals thus forming O(2)-Tl-O(3) bridges along the c axis in the related $Tl_2Ba_2CaCu_2O_8$ and $Tl_2Ba_2Ca_2Cu_3O_{10}$ compounds.[26,27] This strong hybridization is related to very short Tl-O(3) and Tl-O(2) bond distances. The high-energy prepeaks around 530 eV in the O $1s$ absorption edge from the $Tl_2Ba_2CaCu_2O_8$ and $Tl_2Ba_2Ca_2Cu_3O_{10}$ compounds were ascribed to the transitions of O $1s$ electrons to O $2p$ hole states in the O(2) and O(3) sites.[4,28,29]

Because of relatively short distance of about 2 Å between Tl and O(2) atoms along the c axis in the $(Tl_{0.5}Pb_{0.5})Sr_2(Ca_{1-x}Y_x)Cu_2O_7$ compounds, the hybridization of Tl $6s$ and Tl $5d$ with O(2) and O(3) $2p$ orbitals is therefore expected to be very strong. Thus, we would expect the hybridized states of Tl $6s$ and Tl $5d$ with O(2) and O(3) $2p$ orbitals in the $(Tl_{0.5}Pb_{0.5})Sr_2(Ca_{1-x}Y_x)Cu_2O_7$ compounds to contribute the empty conduction band. However, in contrast to the double-thallium-layer compounds, this conduction band does not cross the Fermi level because the compounds for $x>0.6$ are nonconducting. It is therefore believed that one possible contribution to the peak at ~530 eV is due to the transitions to the O(2)-(Tl,Pb)O(3)-O(2) hybridized states. However, another possible final state associated with the transition at ~530 eV is the upper Hubbard band of the strongly correlated Cu $3d$ states highly hybridized with the O $2p$ states. Such a band has always been assumed to exist since the parent compounds of the cuprate superconductors are known to be antiferromagnetic insulators with strong on-site correlation on the copper sites.[30] Therefore, the broad peak at ~530 eV may be due to a superposition of unoccupied O $2p$ states originating from the O(2) and O(3) atoms and the upper Hubbard band related to the CuO_2 planes.

The absorption features shown in Fig. 3 were analyzed by fitting Gaussian functions to each spectrum. The integrated intensity of the pre-edge peak at ~528.3 eV, normalized against the intensity of main peak at ~537 eV, is plotted as a function of compositional parameter x in Fig. 4. It can be seen from Fig. 4 that the intensity of this pre-edge peak increases linearly with the Ca doping for $0\leqslant x\leqslant 0.5$. This demonstrates clearly that the pre-edge peak at ~528.3 eV derived from O(1) sites in the CuO_2 planes is correlated to the hole concentration induced by the chemical substitution of Ca^{2+} for Y^{3+} in the titled system.

The new electronic state at ~528.3 eV disappears by reducing the sample and by going in the semiconducting phase. It should be pointed out that the system goes through a transition from a semiconductor to a metal-superconductor at $x=0.6$. Therefore, the generation of holes derived from the pre-edge feature at ~528.3 eV near the Fermi level is probably responsible for inducing a transition from a semiconductor to a superconductor. In addition, the intensity of the pre-edge peak at ~528.3 eV closely correlates with the compositional variation of superconducting transition temperature. This leads to conclude that holes generated in the O $2p$ orbitals within the CuO_2 planes play an important role to control the T_c of the titled system.

The peaks at ~532.4 and ~533.8 eV are due to surface contamination since those peaks exhibit a greater intensity in surface-sensitive total-electron yield spectra. Existence of surface contamination has been reported by many research-

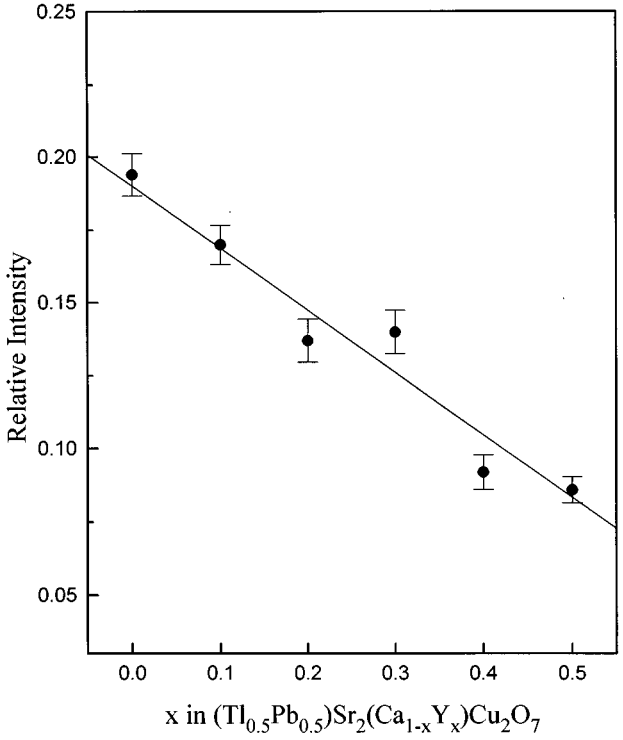

FIG. 6. Dependence on compositional parameter x in $(Tl_{0.5}Pb_{0.5})Sr_2(Ca_{1-x}Y_x)Cu_2O_7$ of the normalized intensity of defect states at 933.1 eV on the Cu sites. The curves are drawn as a guide for the eyes.

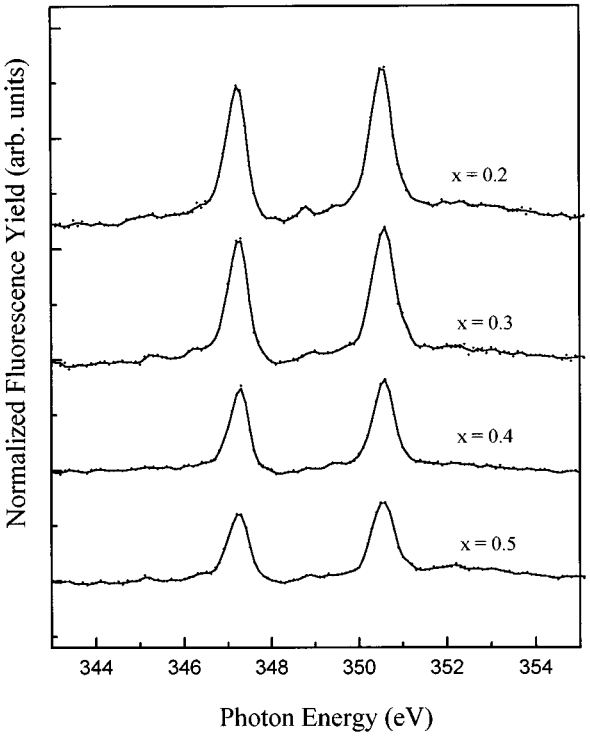

FIG. 7. Calcium L_{23}-edge x-ray-absorption spectra of $(Tl_{0.5}Pb_{0.5})Sr_2(Ca_{1-x}Y_x)Cu_2O_7$ with $x=0.2$, 0.3, 0.4, and 0.5.

ers. According to their photoemission results, Iqbal *et al.* concluded that these peaks are due to absorption of hydrides, water, and CO_2 on surface.[31]

2. Cu *L*-edge XANES

The unoccupied Cu $3d$ states in the $(Tl_{0.5}Pb_{0.5})Sr_2(Ca_{1-x}Y_x)Cu_2O_7$ compounds can be probed by the Cu L-edge x-ray-absorption spectrum. However, contrary to the O $1s$ x-ray-absorption spectrum, the absorption spectrum in the Cu L edge exhibits strong excitonic character due to a significant overlap of the final $3d$ wave functions with those of the $2p$ core hole. Therefore no direct information on the partial density of unoccupied Cu $3d$ states can be obtained. However, some useful information on the occupation of the ground and final states can be extracted from the experimental Cu L-edge x-ray-absorption spectrum.

The Cu L_{23}-edge x-ray-absorption near-edge-structure total-fluorescence-yield spectra of $(Tl_{0.5}Pb_{0.5})Sr_2(Ca_{1-x}Y_x)Cu_2O_7$ ($x=0$–0.9) at room temperature in the energy range of 926–956 eV are shown in Fig. 5. For $x=0.9$, the Cu L_{23}-edge absorption spectrum shows two narrow peaks centered at 931.3 and 951.1 eV, respectively. In the Cu L_{23}-edge absorption spectrum of CuO, a white line at 931.2 eV and satellite structure at 937 eV are observed corresponding to transitions to $(2p_{3/2})^{-1}3d^{10}$ and $(2p_{3/2})^{-1}3d^{9}4s$ final states, respectively, where $(2p_{3/2})^{-1}$ denotes a $2p_{3/2}$ hole.[32] Therefore, the absorption peaks at 931.3 and 951.1 eV shown in Fig. 5 are ascribed to transitions from the $Cu(2p_{3/2,1/2})3d^9$-$O(2)p^6$ ground-state configuration (formal Cu^{2+} state) to the $Cu(2p_{3/2,1/2})^{-1}3d^{10}$-$O(2)p^6$ excited state.

For samples with decreasing x (i.e., increasing hole concentration), the absorption peaks become asymmetric and two new features appear to exhibit at the high-energy side of the main peak. From the curve-fitting analysis, the new features are found to center at about 933.1 and 952.9 eV, respectively. In Fig. 6 the area under this high-energy shoulder, normalized against the area under the L_3 peak at 931.3 eV, is plotted as a function of the compositional parameter x. The areas were estimated by fitting the main peak and the shoulder by Gaussian functions. As seen from Fig. 6, the normalized intensity of this high-energy shoulder shows a linear increase with increasing the Ca concentration.

It is noted that the curve in Fig. 6 resembles the behavior for the pre-edge peak at ~528.3 eV in the O K-edge absorption spectra shown in Fig. 4. Therefore, it is suggested that these high-energy structures may originate from the O $2p$ hole states and are assigned as transitions from the $Cu(2p_{3/2,1/2})3d^9L$ ground state (formal Cu^{3+} state) to the $Cu(2p_{3/2,1/2})^{-1}3d^{10}L$ excited state, where L denotes the O $2p$ ligand hole.[33,34] Increasing the Ca concentration in the $(Tl_{0.5}Pb_{0.5})Sr_2(Ca_{1-x}Y_x)Cu_2O_7$ system is to induce more $2p$ holes on the oxygen sites (i.e., produce the $Cu3d^9L$ defect states) and consequently increase in intensity at high-energy shoulder in Cu L-edge absorption spectra. Similar to the defect states in O $1s$ XANES spectra, these electronic states disappear by reducing the sample and by transferring to the semiconducting or insulating phase. Because there is only one type of Cu site in the unit cell for the series of $(Tl_{0.5}Pb_{0.5})Sr_2(Ca_{1-x}Y_x)Cu_2O_7$ compounds (i.e., no Cu-O chains as in $YBa_2Cu_3O_{7-\delta}$), these high-energy features in the Cu L-edge absorption spectra can be apparently identified as the result of the hole doping in the O(1) sites within the CuO_2 layers due to the chemical substitution of Ca^{2+} for

Y^{3+}. The close resemblance between the high-energy features in the Cu L-edge absorption spectra and the pre-edge peak at ~528.3 eV in the O 1s absorption spectra gives an evidence in support of the suggestion that the pre-edge peak at ~528.3 eV originates from the O(1) sites within the CuO_2 planes.

The Ca L_{23}-edge x-ray-absorption spectra of $(Tl_{0.5}Pb_{0.5})Sr_2(Ca_{1-x}Y_x)Cu_2O_7$ with $x=0.2$, 0.3, 0.4, and 0.5 are shown in Fig. 7. Two strong peaks at 347.2 and 350.6 eV originate from the transitions of the Ca $2p_{1/2}-2p_{3/2}$ spin-orbit splitting states into the empty d states. The overall shape of the Ca L-edge x-ray-absorption spectrum is the same for compounds with different x values, but its intensity changes roughly in line with the Ca content in these compounds.

IV. CONCLUSION

In this study, we perform high-resolution O K-edge and Cu L_{23}-edge x-ray-absorption near-edge-structure measurements for the series of $(Tl_{0.5}Pb_{0.5})Sr_2(Ca_{1-x}Y_x)Cu_2O_7$ compounds ($x=0$–0.9) using a bulk-sensitive total-fluorescence-yield technique. Near the O 1s edge, the pre-edge peak at ~528.3 eV is ascribed to the core-level excitations of O 1s electrons to O 2p holes located in the CuO_2 planes. The intensity of this pre-edge peak increases linearly with the Ca doping for $0\leqslant x\leqslant 0.5$. This indicates that the effect of chemical substitution of Ca^{2+} for Y^{3+} is to induce hole states in the CuO_2 planes near the Fermi level. The intensity of this pre-edge peak closely correlates with the compositional variation of superconducting transition temperature, showing that holes generated in the O 2p orbitals within the CuO_2 planes play an important role to control the T_c of the titled system. In the Cu L-edge absorption spectra, high-energy shoulders at 933.1 and 952.9 eV are assigned to the transitions from the $Cu(2p_{3/2,1/2})3d^9L$ ground state to the $Cu(2p_{3/2,1/2})^{-1}3d^{10}L$ excited state, where L denotes the O 2p ligand hole. The normalized intensity of these defect states shows a linear increase with increasing the Ca concentration. According to the present XANES study, it is interpreted that the transition from superconductors to semiconductors of $(Tl_{0.5}Pb_{0.5})Sr_2(Ca_{1-x}Y_x)Cu_2O_7$ as the increase of the Y content results mainly from the decrease of the hole content from the CuO_2 planes.

ACKNOWLEDGMENTS

We would like to thank Shih-Chang Chung and all the members at SRRC for their technical support. This research is financially supported by SRRC and National Science Council of the Republic of China.

[1] J. B. Torrance, Y. Tokura, A. I. Nazzal, A. Bezinge, T. C. Huang, and S. S. P. Parkin, Phys. Rev. Lett. **61**, 1127 (1988).
[2] H. Romberg, M. Alexander, N. Nücker, P. Adelmann, and J. Jink, Phys. Rev. B **42**, 8768 (1990).
[3] C. T. Chen, F. Sette, Y. Ma, M. S. Hybertsen, E. B. Stchel, W. M. C. Foulkes, M. Schluter, S. W. Cheong, A. S. Cooper, L. W. Rupp, Jr., B. Batogg, Y. T. Soo, Z. H. Ming, A. Krol, and Y. H. Kao, Phys. Rev. Lett. **66**, 104 (1991).
[4] J. Fink, N. Nücker, E. Pellegrin, H. Romberg, M. Alexander, and M. Kunpfer, J. Electron Spectrosc. Relat. Phenom. **66**, 395 (1994).
[5] M. A. Subramanian, C. C. Torardi, J. Gopalakrishnan, P. L. Gai, P. L. Calabrese, T. R. Askew, R. B. Flippen, and A. W. Sleight, Science **242**, 249 (1988).
[6] C. N. R. Rao, A. K. Ganguli, and R. Vijayaraghavan, Phys. Rev. B **40**, 2562 (1989).
[7] G. Mante, Th. Schmalz, R. Manzke, M. Skibowski, M. Alexander, and J. Fink, Surf. Sci. **269/270**, 1071 (1992).
[8] B. Raveau, C. Michel, M. Hervieu, D. Groult, and J. Provost, J. Solid State Chem. **85**, 181 (1990).
[9] R. S. Liu, P. P. Edwards, Y. T. Huang, S. F. Wu, and P. T. Wu, J. Solid State Chem. **86**, 334 (1990).
[10] R. S. Liu and P. P. Edwards (unpublished).
[11] J. Yuan, L. M. Browa, W. Y. Liang, R. S. Liu, and P. P. Edwards, Phys. Rev. B **43**, 8030 (1991).
[12] R. A. Rosenberg, J. K. Simons, S. P. Frigo, K. Tan, and J. M. Chen, Rev. Sci. Instrum. **63**, 2193 (1992).
[13] H. M. Meyer, III, T. J. Wagnener, J. H. Weaver, and D. S. Ginley, Phys. Rev. B **39**, 7243 (1989).
[14] P. Kuper, G. Kruizinga, J. Ghijsen, M. Grioni, P. J. Weijs, F. M. F. De Groot, G. A. Sawatzki, H. Verweij, L. F. Feiner, and H. Petersen, Phys. Rev. B **38**, 6483 (1988).
[15] N. Nücker, J. Fink, J. C. Fuggle, P. J. Durham, and W. M. Temmerman, Phys. Rev. B **37**, 5158 (1988).
[16] R. S. Liu and P. P. Edwards, Mater. Sci. Forum **130**, 435 (1993).
[17] E. Pellegrin, J. Fink, C. T. Chen, Q. Xiong, Q. M. Lin, and C. W. Chu, Phys. Rev. B **53**, 2767 (1996).
[18] R. P. Vasquez, M. Rupp, A. Gupa, and C. C. Tsuei, Phys. Rev. B **51**, 15 657 (1995).
[19] E. Pellegrin, N. Nücker, J. Fink, S. L. Molodtsov, A. Gutiérrez, E. Navas, O. Strebel, Z. Hu, M. Domke, G. Kaindl, S. Uchida, Y. Nakamura, J. Markl, M. Klauda, G. Saemann-Ischenko, A. Krol, J. L. Peng, Z. Y. Li, and R. L. Greene, Phys. Rev. B **47**, 3354 (1993).
[20] A. R. Moodenbaugh and D. A. Fischer, Physica C **230**, 177 (1994).
[21] N. Nücker, E. Pellegrin, P. Schweiss, J. Fink, S. L. Molodtsov, C. T. Simmons, G. Kaindl, W. Frentrup, A. Erb, and Müller-Vogt, Phys. Rev. B **51**, 8529 (1995).
[22] C. T. Chen, L. H. Tjeng, J. Kwo, H. L. Kao, P. Rudolf, F. Selle, and R. M. Fleming, Phys. Rev. Lett. **68**, 2543 (1992).
[23] H. M. Meyer, III, T. J. Wagnener, J. H. Weaver, and D. S. Ginley, Phys. Rev. B **38**, 7144 (1988).
[24] A. Fujimori, Y. Tokura, H. Eisaki, H. Takagi, S. Uchida, and E. Takayama-Muromachi, Phys. Rev. B **42**, 325 (1990).
[25] W. Wruke, F. J. Himpsel, G. V. Chandrashekar, and M. W. Shafer, Phys. Rev. B **39**, 7328 (1989).
[26] P. Marksteiner, J. Yu, S. Massidda, A. J. Freeman, J. Reinger, and P. Weinberger, Phys. Rev. B **39**, 2894 (1989).
[27] R. V. Kasowski, W. Y. Hsu, and F. Herman, Phys. Rev. B **38**, 6470 (1988).
[28] E. Pellegrin, N. Nücker, J. Fink, C. T. Simmons, G. Kaindl, J.

Bernhard, K. F. Renk, G. Kumm, and K. Winzer, Phys. Rev. B **48**, 10 520 (1993).

[29] H. Romberg, N. Nücker, M. Alexander, J. Fink, D. Hahn, T. Zetterer, H. H. Otto, and K. F. Renk, Phys. Rev. B **41**, 2609 (1990).

[30] D. Vaknin, S. K. Shiha, D. E. Moneton, D. C. Johnston, J. M. Newsam, C. R. Safiva, and H. E. King, Jr., Phys. Rev. Lett **58**, 2802 (1987).

[31] Z. Iqbal, E. Leone, R. Chin, A. J. Signorelli, A. Bose, and H. Eckhardt, J. Mater. Res. **2**, 768 (1987).

[32] M. Grioni, J. B. Goedkoop, R. Schoorl, F. M. F. de Groot, J. C. Fuggle, F. Schafers, E. E. Koch, G. Rossi, J. M. Esteva, and R. C. Karnatak, Phys. Rev. B **39**, 1541 (1989).

[33] A. Bianconi, A. Congiu Castellano, M. De Santis, P. Rudolf, P. Lagarde, A. M. Flank, and A. Marcelli, Solid State Commun. **63**, 1009 (1987).

[34] D. D. Sarma, O. Strebel, C. T. Simmons, U. Neukirch, and G. Kaindl, Phys. Rev. B **36**, 8285 (1988).